Accelerating Flow Encoded MRI by Exploiting Vector Field Divergence Regularization

Claudio Santelli[1,2], Michael Loecher[3], Julia Busch[2], Oliver Wieben[3,4], Tobias Schaeffter[1], and Sebastian Kozerke[1,2]

[1]*Imaging Sciences and Biomedical Engineering, King's College London, London, United Kingdom,* [2]*Institute for Biomedical Engineering, University and ETH Zurich, Zurich, Switzerland,* [3]*Department of Medical Physics, University of Wisconsin-Madison, Wisconsin, United States,* [4]*Department of Radiology, University of Wisconsin-Madison, Wisconsin, United States*

Target Audience Physicists and engineers interested in image reconstruction of flow encoded MRI data.

Purpose Long acquisition times and image phase inaccuracies are the main concerns in time-resolved 3D phase-contrast (PC) MRI. Standard compressed sensing (CS) [1] scan acceleration techniques use sparsifying transforms designed for object magnitude with smooth background phase. A CS reconstruction framework separately regularizing magnitude and phase has been presented [2]. The principle of incorporating the divergence-free condition of 3D blood flow directly into the reconstruction process has been recently proposed [3]. In the present work, an efficient algorithm penalizing divergence and curl using finite-difference (FD) derivative filters is presented together with a variant of iterative divergence-free Wavelet (DFW) thresholding [4].

Theory For 4-point PC flow measurements [5], minimizing the error functional $f(\mathbf{m},\boldsymbol{\phi}_v) = \|\mathbf{d}-\mathbf{E}(\mathbf{m}\circ e^{i\boldsymbol{\phi}_0}\circ e^{i\boldsymbol{\phi}_v})\|_2^2 + \lambda_m\|\boldsymbol{\Psi}_m\mathbf{m}\|_1 + \lambda_\phi\|\boldsymbol{\Psi}_\phi\mathbf{K}_v\boldsymbol{\phi}_v\|_1$ (1) allows separate reconstruction of magnitude $\mathbf{m}\in\mathbb{R}^{3N}$ and velocity induced phase $\boldsymbol{\phi}_v\in\mathbb{R}^{3N}$ of the flow encoded segments (with elementwise vector product $\circ$, k-space data vector $\mathbf{d}\in\mathbb{C}^{3M}$, encoding matrix $\mathbf{E}$, regularization parameters $\lambda_{m,\phi}$, magnitude sparsifyer $\boldsymbol{\Psi}_m$, velocity vector field operator $\boldsymbol{\Psi}_\phi$ and diagonal velocity encoding matrix $\mathbf{K}_v$). The vector $\boldsymbol{\phi}_0$ captures the reference segment's phase and background correction (e.g. concomitant fields or eddy currents) maps. During iteration step $k+1$, f is alternately minimized with respect to phase and magnitude: $\boldsymbol{\phi}_v^{k+1} = \text{argmin}_{\boldsymbol{\phi}_v} f(\mathbf{m}^k,\boldsymbol{\phi}_v)$ (2), $\mathbf{m}^{k+1} = \arg\min_{\mathbf{m}} f(\mathbf{m},\boldsymbol{\phi}_v^{k+1})$ (3). For the FD method, the flow field operator is composed of divergence and curl calculations with relative weight $\gamma\in\mathbb{R}^{\geq 0}$: $\boldsymbol{\Psi}_\phi = [\boldsymbol{\Psi}_{div}^T \quad \gamma\boldsymbol{\Psi}_{curl}^T]^T$ (4). For DFW implementation, upon 3D Wavelet transformations $\boldsymbol{\Psi}_{x,y,z}$, coefficients are linearly combined using $\mathbf{A}$ resulting in divergence-free and non-divergence-free components [6]: $\boldsymbol{\Psi}_\phi = \mathbf{A}diag(\boldsymbol{\Psi}_x \ \boldsymbol{\Psi}_y \ \boldsymbol{\Psi}_z)$ (5). Fig. 1 illustrates the proposed FD and DFW algorithms with $\mathbf{E}_{\mathbf{m},\boldsymbol{\phi}_0}^k = \mathbf{E}diag(\mathbf{m}^k\circ e^{i\boldsymbol{\phi}_0})$ (12) being the modified encoding matrix and n denoting the sub-step within the $(k+1)$-th outer iteration step.

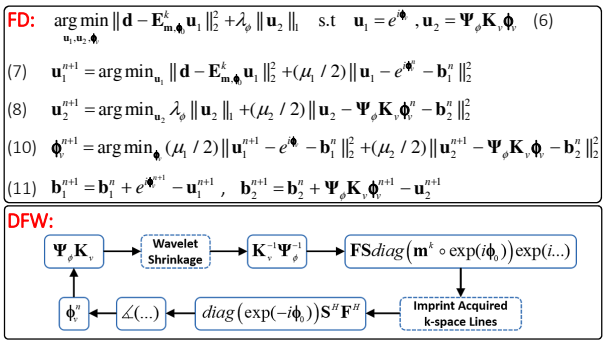

Figure 1 Reconstruction algorithms for phase updates (2). Top: Following [7], equation (2) is reformulated as the constrained problem (6) using auxiliary variables $\mathbf{u}_{1,2}$. Upon reformulation as an unconstrained problem with the Lagrange multiplier vectors $\mathbf{b}_{1,2}$ and tuning parameters $\mu_{1,2}$, alternating minimization with respect to $\mathbf{u}_{1,2}$ and $\boldsymbol{\phi}_v$ including update rules (11) for $\mathbf{b}_{1,2}$ is used. While (7) and (8) can be solved via linear conjugate gradient (CG) and soft-thresholding, respectively, nonlinear CG [2] is employed to solve (10). Bottom: After DFW shrinkage, the resulting phase exponential vector is combined with magnitude and background phase before the data consistency step ($\mathbf{F}$: Fourier Transform, $\mathbf{S}$: Sensitivity weighting). Upon subtraction of $\boldsymbol{\phi}_0$, the phase provides an intermediate solution of $\boldsymbol{\phi}_v$.

Methods 4-point PC MR data were simulated based on CFD data in a U-bend shaped tube with an approximately divergence-free fluid. A simulated 7-element coil array was incorporated. Complex Gaussian noise mimicking an SNR of 15 was added. 3D cine 4-point PC data of the aortic arch (6 coils, 24 heart phases, 42ms temp. res., 322x252x50.75-57.75 mm^3 imaging volumes, 1.75x1.75x1.75 mm^3 voxel size, 10° flip angle, TR/TE = 4.7/2.4 ms) were acquired in 5 healthy volunteers on a 3T Philips Achieva scanner (Philips Healthcare, Best, The Netherlands). Data were retrospectively undersampled (3- and 6-fold) using variable density sampling pattern [1] in the phase encoding plane. Normalized 3D coil sensitivities were estimated from the temporally averaged reference segment using ESPIRiT [8]. An iterative soft-thresholding algorithm [9] leaving the acquired data unchanged was used for standard CS ℓ_1-Wavelet reconstruction. A variant of ℓ_1-POCSENSE [10] fixing image phase was used for the magnitude updates (3). For the reference segment, the phase was ℓ_2-regularized using a gradient operator on the phase exponential: $\|\nabla e^{i\boldsymbol{\phi}_0}\|_2^2$ [2].

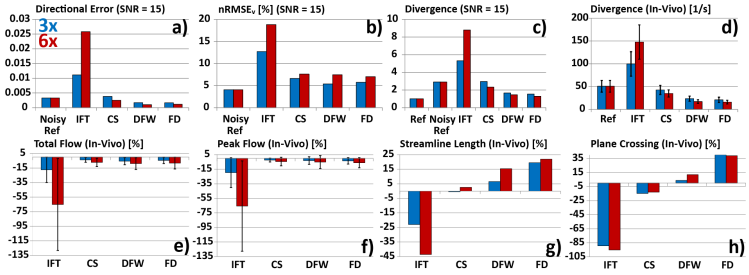

Figure 2 Comparison of directional error **a)**, normalized root mean squared error (nRMSE$_v$) of velocity magnitude **b)** and mean absolute divergence for numerical phantom **c)** and in-vivo **d)** data. **e,f)** Errors in total and peak flow estimation relative to fully sampled reference. **g,h)** Relative change in streamline length and number of streamlines reaching the end of the descending aorta.

Results Fig. 2 shows error, divergence, total and peak flow and streamline quantification results of simulated and in-vivo data (IFT: direct inverse Fourier transformation). Improvements with phase regularization relative to CS are seen in Fig. 2a-d and g-h. Direction-, divergence- and streamline-metrics are found to improve with increased undersampling factor. Fig. 3 illustrates velocity profiles and vectors of numerical and in-vivo data, respectively.

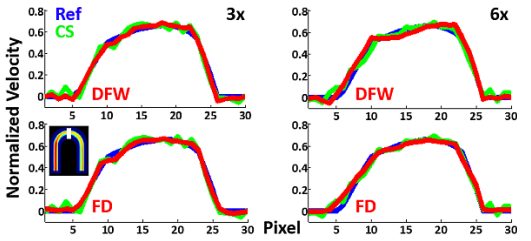

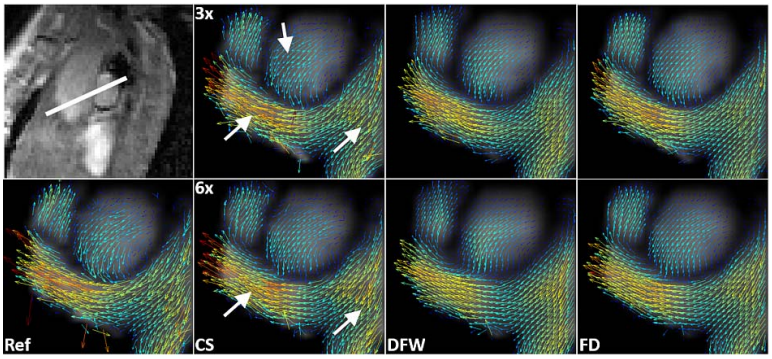

Figure 3 Top: Through-plane velocity profiles across indicated line reconstructed from CFD data. Bottom: In-plane velocity field visualization in the indicated cross-section in a representative healthy subject. The arrows point to differences between CS, DFW and FD reconstructions.

Discussion In this work, reconstruction methods imposing the incompressibility of blood flow have been proposed and applied on simulated and in-vivo 3D PC data. Relative to convex CS, DFW and FD result in reduced directional error and divergence, increased streamline length and improved vector field visualization. With increasing undersampling, reconstructed vector fields are increasingly denoised, thereby favoring direction dependent error metrics at the expense of some underestimation of total and peak flow. In summary, phase regularization is a promising tool to enhance accelerated cine 3D PC-MRI. Future work will include the investigation of optimized sampling patterns, high spatial resolution and data acquisition in patients.

References [1] Lustig M et al. MRM 2007;58(6):1182-1195. [2] Zhao F et al. IEEE TMI 2012;31(9):1713-1723. [3] Loecher M et al. ISMRM 2013:1355. [4] Ong F et al. ISMRM 2014:326. [5] Pelc NJ et al. JMRI 1991;1(4): 405-413. [6] Deriaz E et al. JTurbul 2006;7(3):1-37. [7] Ramani S et al. IEEE TMI 2011;30(3):694-706. [8] Uecker M et al. MRM 2014;71(3):990-1001 2014. [9] Daubechies I et al. CPAM 2004;57(11):1413-1457. [10] Samsonov AA et al. MRM 2004;52(6):1397-1406.